

Atomic physics of channeled ions

Oakley H. Crawford and R. H. Ritchie

Oak Ridge National Laboratory, Oak Ridge, Tennessee 37830

(Received 22 January 1979)

Electronic states of swift channeled ions are studied in terms of a time-dependent effective-Hamiltonian theory. These states are shifted in energy by the electric potential of the perturbed crystal, and transitions among them are induced coherently by the oscillation of the potential. Calculated energies for low-lying states of hydrogenic ions channeled in Au are in reasonable agreement with experimental resonant coherent-excitation spectra.

I. INTRODUCTION

Channeling, the passage of swift projectiles through crystals by way of channels bounded by strings or planes of atoms, has figured in many studies in recent years.¹ However, little attention has been paid to the internal degrees of freedom of channeling ions.² Recently, electronic spectra of such ions have been measured^{3,4} using resonant coherent excitation,⁵ giving to the theory of their electronic states new interest and importance.

A time-dependent effective-Hamiltonian formalism is presented for channeled ions, which describes the energies of low-lying electronic states, the coherent transitions between these states, and the decay of coherence. Electronic wave functions and energies are calculated for various one-electron ions axially channeled in Au, and the theoretical resonant coherent-excitation spectra are compared with experimental results.^{3,4}

Kutcher and Mittleman,² in a 1975 paper having a similar title to the present one, presented a theory of hydrogen-like ions channeling at high velocity and predicted wave functions and binding energies of He⁺ and H channeling in Na at the high-velocity (nonrelativistic) limit. Our treatment resembles theirs in using an effective-Hamiltonian approach and has the same high-velocity limit, but there are basic differences, which are important for the present calculations. These differences occur in the choices of P space for which the effective Hamiltonian is defined, in the retention in the present case of the variations in the potential along the channel direction, and in the treatments of polarization of the crystal.

II. TIME-DEPENDENT EFFECTIVE-HAMILTONIAN THEORY

Consider an ion channeling at high velocity, $v > Zv_0$, where Z and v_0 are the atomic number and the Bohr velocity,⁶ respectively. The nucleus

is assumed to follow a prescribed classical trajectory while the wave function for the remainder of the system evolves according to the time-dependent Schrödinger equation

$$\left(i\hbar \frac{\partial}{\partial t} - H \right) \Psi(\vec{r}_a, \vec{r}_c, t) = 0, \quad (1)$$

where \vec{r}_a and \vec{r}_c represent all the position coordinates of the ion's electrons, and the particles of the crystal, respectively, relative to an origin fixed to the crystal. The Hamiltonian H is the sum of the Hamiltonians H_a and H_c of the free ion and the unperturbed crystal, respectively, and the ion-crystal interaction V :

$$H = H_a(\vec{r}_a, t) + H_c(\vec{r}_c) + V(\vec{r}_a, \vec{r}_c, t). \quad (2)$$

The time dependence indicated for H_a and V arises from their dependences on the position of the ion.

If the ion has a small enough radius, its interaction $V(\vec{r}_a, \vec{r}_c, t)$ with the crystal is approximately the interaction, call it $U(\vec{r}_c, t)$, of the equivalent point charge with the crystal. Now the Hamiltonian H_0

$$H_0 = H_a(\vec{r}_a, t) + H_c(\vec{r}_c) + U(\vec{r}_c, t) \quad (3)$$

obtained from H by replacing V with U has the advantage of being separable in \vec{r}_a and \vec{r}_c , as well as being a reasonable approximation to H . Therefore a useful basis for solution of Eq. (1) is

$$\xi_{iI} = \chi_I(\vec{r}_c, t) \phi_i(\vec{r}_a, t), \quad (4)$$

where the χ_I are an orthonormal set of wave functions of a crystal perturbed by a channeling point charge

$$\left(i\hbar \frac{\partial}{\partial t} - H_c - U \right) \chi_I = 0, \quad (5)$$

and where the ϕ_i are normalized eigenfunctions of H_a , with eigenvalues ϵ_i . Let the ϕ_i be indexed in order of increasing energy ($\epsilon_j \geq \epsilon_i$ if $j > i$), and

have appropriate time-dependent phase factors so that

$$\left(i\hbar\frac{\partial}{\partial t} - H_a\right)\phi_i = (\epsilon_i - H_a)\phi_i = 0. \quad (6)$$

These product functions form a complete set, and satisfy a time-dependent Schrödinger equation with Hamiltonian H_0 :

$$\left(i\hbar\frac{\partial}{\partial t} - H_0\right)\xi_{II} = 0. \quad (7)$$

Exchange of electrons of the ions with those of the crystal may safely be ignored.²

Consider the time evolution of a system in which, at some initial time t_0 , the ion is in a low-lying state, specifically some linear combination of the lowest n ϕ_i functions, while the crystal is in some arbitrary state χ_I . Define time-dependent projection operators P and Q

$$\begin{aligned} P(t) &= \sum_{i=1}^n |\xi_{II}(t)\rangle\langle\xi_{II}(t)| \\ &= \sum_{i=1}^n |\chi_i(t)\phi_i(t)\rangle\langle\chi_i(t)\phi_i(t)| \end{aligned} \quad (8)$$

and

$$Q(t) = 1 - P(t). \quad (9)$$

The wave function Ψ will evolve in P space, and will develop a Q component as time goes on, because of the influence of the term $H' = H - H_0$.

An equation for the evolution of the P -space part of the wave function of the above system may be derived, if Eq. (1) is written as two equations

$$P\left(i\hbar\frac{\partial}{\partial t} - H\right)(P+Q)\Psi = 0, \quad (10)$$

$$Q\left(i\hbar\frac{\partial}{\partial t} - H\right)(P+Q)\Psi = 0 \quad (11)$$

and use is made of the commutators,

$$\left[P, i\hbar\frac{\partial}{\partial t}\right] = -\left[Q, i\hbar\frac{\partial}{\partial t}\right] = [P, H_0]. \quad (12)$$

The solution of Eq. (11) for $Q\Psi$, subject to the initial condition $Q\Psi = 0$ at time t_0 , is

$Q(t)\Psi(t)$

$$= \int_{t_0}^{\infty} dt' G_{QQ}^*(t, t') Q(t') H'(t') P(t') \Psi(t') / \hbar, \quad (13)$$

where G_{QQ}^* is the retarded Green's function which

satisfies the equation

$$\left(i\frac{\partial}{\partial t} - (H_0 + QH'Q)/\hbar\right) G_{QQ}^*(t, t') = I\delta(t - t') \quad (14a)$$

with initial condition

$$G_{QQ}^*(t, t') = 0 \text{ if } t < t', \quad (14b)$$

where I stands for the unit operator.⁷ With the above result for $Q\Psi$, Eq. (10) takes the desired form,

$$\left(i\hbar\frac{\partial}{\partial t} - H_{\text{eff}}\right) P\Psi = 0 \quad (15)$$

in which the effective Hamiltonian is

$$H_{\text{eff}} = H_0 + PH'P - \frac{1}{2}i\hbar\Gamma, \quad (16)$$

where the last term is

$$-\frac{1}{2}i\hbar\Gamma = PH'Q \int_{t_0}^{\infty} dt' G_{QQ}^* QH'P / \hbar, \quad (17)$$

where the time argument t' is understood for the operand of G^+ , as in Eq. (13). The effective Hamiltonian is nonlocal both in space and in time, because of Γ .

A calculation discussed in Sec. IV shows that the Hermitian part of the last term, $-\frac{1}{2}i\hbar\Gamma$, in H_{eff} is negligible compared with $PH'P$ for $Z \geq 6$, and $v > Zv_0$. In addition, we argue that, at high ion velocity ($v \gg Zv_0$), $-\frac{1}{2}i\hbar\Gamma$ is mostly absorptive. The term in question involves a $P \rightarrow Q$ interaction at time $t' < t$, a propagation in Q space from t' to t , and $Q \rightarrow P$ interaction at time t , summed over all $t' < t$. Since the limit of $G_{QQ}^*(t, t')$ as t' approaches t from below is $-iI$, the contribution to the right-hand side of Eq. (17) from the time element dt' running from $t - dt'$ to t approaches $-iPH'QH'P dt' / \hbar = -i(QH'P)^\dagger QH'P dt' / \hbar$ for small dt' . This contribution is all absorptive, as the operator multiplying $-i$ is positive. (We note in passing that it is local in time.) It follows that the Hermitian part, if any, of $-\frac{1}{2}i\hbar\Gamma$ requires interactions at times t' and t removed from each other. We argue below that at high enough velocity, separated interactions are negligible, compared with those occurring closer in time, so that the Hermitian part of $-\frac{1}{2}i\hbar\Gamma$ decreases relative to the absorptive part.

The operator $H' = V - U$ has the following representation in coordinate space

$$H' = -\sum_{ac} eq_c \left[\frac{1}{|\vec{r}_c - \vec{r}_a|} - \frac{1}{|\vec{r}_c - \vec{R}(t)|} \right],$$

where q_c is the charge of the c th particle in the crystal, and $\vec{R}(t)$ is the (prescribed) position of

the ion. In a multipole expansion with respect to the ion position, the leading term in H' at large distance is the dipole term,

$$-\sum_a e(\vec{r}_a - \vec{R}) \cdot \sum_c q_c (\vec{r}_c - \vec{R}) / |\vec{r}_c - \vec{R}|^3.$$

Thus, at large distance $|\vec{r}_c - \vec{R}|$ from the ion, H' , considered as a function of the coordinates of the crystal's particles, falls off as the square of the distance. Therefore, the disturbances of the crystal which are caused by H' are localized, at the time they occur, near the position of the ion. At high enough velocity such that the ion quickly outruns the disturbance, that part of $QH'P$ which involves a transition $\chi_i \rightarrow \chi_k (k \neq i)$ in the crystal contributes to essentially only the absorptive part of $-\frac{1}{2}i\hbar\Gamma$. Those interactions $QH'P$ with that part of Q space in which the ion is excited, but not the crystal, require separate consideration. We assume that n , the number of ion states included in the definition of P space, is chosen to be sufficiently large that ions excited to $\phi_m (m > n)$ will soon excite the crystal⁸ (through $QH'Q$ in the propagator), the result being absorption from P space as above.

It follows that Γ is asymptotically a positive operator, local in time, at high velocity, so that $-\frac{1}{2}i\hbar\Gamma$ is asymptotically purely absorptive. The Hermitian part of $-\frac{1}{2}i\hbar\Gamma$ decreases with velocity, both in an absolute sense, and relative to the absorptive part, and relative to $PH'P$.

We may write $P\Psi$ in a separated form

$$P\Psi = \chi_i p f, \quad (18)$$

where f is an unknown function of the coordinates, \vec{r}_a , of the atomic electrons, and p projects onto the space of n atomic bound states, i.e., is given by Eq. (8) with $|\chi_i\rangle$ and $\langle\chi_i|$ omitted. Then, Eq. (15) reduces to Schrödinger-like equation for pf ,

$$\left[i\hbar \frac{\partial}{\partial t} - h_{\text{eff}} \right] pf = 0, \quad (19)$$

where the effective atomic Hamiltonian, h_{eff} , is

$$h_{\text{eff}} = H_a + p(\chi_i | H' \chi_i) p - \frac{1}{2}i\hbar p(\chi_i | \Gamma \chi_i) p, \quad (20)$$

in which the integration implied by those scalar products notated with parentheses extends only over the crystal coordinates. Now, $(\chi_i | H' \chi_i)$ is given by

$$\begin{aligned} (\chi_i | H' \chi_i) &= \sum_a \left[-e(\chi_i | \sum_c q_c |\vec{r}_a - \vec{r}_c|^{-1} \chi_i) \right. \\ &\quad \left. + e(\chi_i | \sum_c q_c |\vec{R} - \vec{r}_c|^{-1} \chi_i) \right] \\ &= \sum_a \left[-e\Phi(\vec{r}_a, t) + e\Phi(\vec{R}, t) \right], \end{aligned}$$

where $\Phi(\vec{r}, t)$ is the expectation value (with respect to the perturbed crystal wave function χ_i) of the electric potential at point \vec{r} and time t in the crystal, and where the explicit time dependence arises from the change with time of χ_i . That part of $(\chi_i | H' \chi_i)$ which depends on the coordinates of the ion's electrons is, therefore, $-e\sum_a \Phi(\vec{r}_a, t)$. The other term is irrelevant to the ensuing work, as it is a function of time alone. Omitting that term, the effective Hamiltonian becomes

$$h_{\text{eff}} = H_a - ep\Phi p - \frac{1}{2}i\hbar\gamma, \quad (21)$$

where $\gamma = (\chi_i | \Gamma \chi_i)$. Here and in the following, Φ means $\sum_a \Phi(\vec{r}_a, t)$.

Let us express the above results, Eqs. (19) and (21), in an interaction picture. In order to avoid secular terms in the Hermitian part of the interaction matrix, first linearly transform the basis to the (time-independent orthonormal) one which diagonalizes that part, $p(H_a - e\Phi_{DC})p$, of h_{eff} which is time invariant and Hermitian.

$$p(H_a - e\Phi_{DC})p\psi_i = E_i\psi_i, \quad i = 1, 2, \dots, n, \quad (22)$$

where Φ_{DC} is the time average of Φ , measured relative to the nucleus of the moving ion:

$$\Phi_{DC}(\vec{r}') \equiv \lim_{T \rightarrow \infty} \frac{1}{T} \int_0^T dt \Phi[\vec{R}(t) + \vec{r}', t].$$

Then, upon expanding pf as follows,

$$pf = \sum_i^n C_i \psi_i e^{-iE_i t/\hbar}, \quad (23)$$

the effective Schrödinger equation, Eq. (19) becomes

$$\begin{aligned} i\hbar \frac{dC_i}{dt} &= \sum_{j=1}^n [-e \langle i | \Phi_{AC} | j \rangle \\ &\quad - \frac{1}{2}i\hbar \gamma_{ij}] e^{i(E_i - E_j)t/\hbar} C_j, \quad i = 1, 2, \dots, n, \quad (24) \end{aligned}$$

where $\Phi_{AC} = \Phi - \Phi_{DC}$, and where matrix elements are in the ψ basis.

The interpretation of the above result is simple and direct. Consider the effective Hamiltonian h_{eff} (Eq. 21). The potential $-ep\Phi_{DC}p$ (which is con-

stant in time) mixes the n atomic states of p space and perturbs their energies. The new states are the ψ_i with energies E_i . The oscillating potential $-ep\Phi_{AC}p$ causes coherent transitions between these states, and $-\frac{1}{2}i\hbar\gamma$ causes loss of coherence and lifetime broadening.

The spectra of ions passing through solids may be observed in emission, if the radiative lifetime is much shorter than the time the ions spend in the crystal. This has been done by Bell *et al.*⁹ for the $(1s2p)^1P_1 - (1s^2)^1S_0$ transition in helium-like sulphur, S^{14+} , in aluminum. The projectiles were not channeled, in which case the time average $\Phi_{0,DC}$ of the static potential is zero, and the ion's electronic energies (Eq. 22) are perturbed by only the polarization potential. Such an interpretation was offered by Bell *et al.*⁹ and by Jakubassa¹⁰ for the observed line shift.

III. RESONANT COHERENT EXCITATION

The oscillating potential Φ_{AC} of the crystal itself may be used to resonantly excite swift ions in single crystals. It follows from Eq. (24) that resonant coherent $i-j$ transitions may occur when one of the angular frequencies $\omega_{\vec{k}}$ of $\langle i | \Phi_{AC} | j \rangle$ is in resonance with the energy difference, i.e., when both the resonance condition

$$\omega_{\vec{k}} \simeq (E_i - E_j)/\hbar \quad (25)$$

and selection rules⁴ are satisfied.¹¹ This possibility was predicted by Okorokov,⁵ for axially channeled ions. References to other work are given in Ref. 4.

The present treatment applies not only to both axial and planar channeling, but to projectile trajectories in arbitrary directions. Channeling is therefore not a necessary requirement for resonant coherent excitation. This is a good place to note that a long coherence time is necessary for sharp resonances. Coherence times increase with increasing velocity and increasing atomic number,⁸ and are longer for channeled ions than for unchanneled ones.

The angular frequencies $\omega_{\vec{k}}$ of Φ_{AC} , for an ion moving with velocity \vec{v} , are determined by the crystal symmetry and lattice parameters, and take only the values

$$\omega_{\vec{k}} = \vec{g} \cdot \vec{v}, \quad (26)$$

where \vec{g} is a reciprocal-lattice vector. For gold, which is face-centered cubic, with lattice constant a , take the conventional cubic unit cell and Cartesian basis. Then these vectors are

$$\vec{g} = (2\pi h/a, 2\pi k/a, 2\pi l/a), \quad (27)$$

the integers h , k , and l taking all values restric-

ted such that no even integer is combined with any odd integer in the same vector.¹²

It follows that the p -space electronic spectra of channeled ions may be measured by observing at what velocities resonant coherent transitions occur. Sections IV and V contain calculations of these spectra from the above effective Hamiltonian theory, and comparisons with experimental values.

IV. CALCULATIONS

Calculations of electronic energies E_i of one-electron ions moving along trajectories centered in the $\langle 100 \rangle$ and $\langle 111 \rangle$ axial channels and in the $\{100\}$ planar channel of Au will be described. These channels are illustrated in Fig. 1, which gives different views, all to the same scale, of a simple face-centered cubic lattice. Only the $1s$, $2s$, and $2p$ hydrogenic states are included in P space. The energies are the five eigenvalues of the operator $p(H_a - e\Phi_{DC})p$ as discussed above, the Hermitian part of the remainder $-\frac{1}{2}i\hbar\Gamma$ of the effective Hamiltonian being negligible (see below).

We require matrix elements of expectation values $\Phi(\vec{r}, t)$ of the electric potential in a crystal which is interacting with a moving point charge (at the location of the channeled ion) of charge Q . The fact that stopping power varies with the charge Q approximately as Q^2 suggests that a first-order perturbation calculation of Φ is adequate for the present purposes. Accordingly, take

$$\Phi = \Phi_0 + \Phi_1, \quad (28)$$

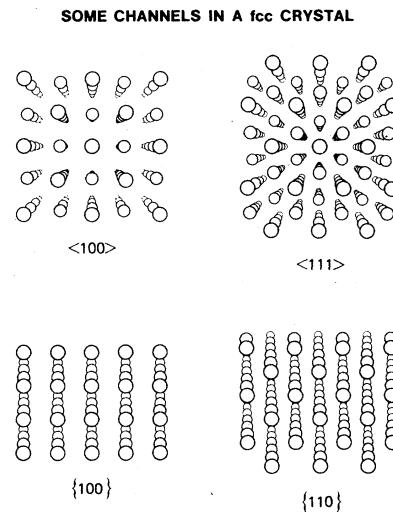


FIG. 1. Perspective drawings, to the same scale, of a simple fcc crystal, showing $\langle 100 \rangle$ and $\langle 111 \rangle$ axial channels, and $\{100\}$ and $\{110\}$ planar channels. The distance between centers of adjacent $\langle 100 \rangle$ strings of

where Φ_0 and Φ_1 are the expectation values of the unperturbed potential, and of the polarization potential (first order in U), respectively.

The potential Φ_0 is taken to be a sum of atomic potentials, averaged over vibrations. Au is face-centered cubic, and we take the conventional cubic unit cell. The origin of space coordinates is the center of one of the atoms, and orthogonal u , v , and w axes are directed toward other atoms at distances a , the lattice constant, from the origin. Thus, Φ_0 as a function of position \vec{r} is

$$\Phi_0(\vec{r}) = \sum_{\vec{g}} \Phi_0(g) e^{i\vec{g}\cdot\vec{r}}, \quad (29)$$

where the sum is over reciprocal-lattice vectors \vec{g} , defined by Eq. (27). The coefficients $\Phi_0(g)$ are single-atom factors $\Phi_a(g)$ (proportional to electron scattering form factors) multiplied by Debye-Waller factors:

$$\Phi_0(g) = \Phi_a(g) e^{-Mg^2}, \quad (30)$$

where

$$\Phi_a(g) = \frac{16\pi}{ga^3} \int_0^\infty \sin(gr) \Phi_{\text{at.}}(r) r dr, \quad (31)$$

where $\Phi_{\text{at.}}$ is the expectation value of the electric potential in a single Au atom, which we take from a Hartree-Dirac-Slater calculation with Wigner-Seitz boundary conditions (radius, 3.011 Bohr radii) described by Tucker *et al.*¹³ The last factor in Eq. (30) arises from averaging the potential over lattice vibrations, assuming independent isotropic Gaussian probability density distributions for the atoms. The exponential factor M is found to be

$$M = \frac{1}{6} \bar{u}^2, \quad (32)$$

where \bar{u}^2 is the mean-square atomic displacement, which is¹⁴ 0.0188 Å² for Au at room temperature.

Define $\Phi_{0,DC}$ as the time-invariant part of Φ_0 from the reference of the moving ion. When $\Phi_0(\vec{r})$ is expressed as a function of position \vec{r}' relative to that of the moving nucleus, $\vec{R}(t)$, and averaged over time, one finds, for the straight line trajectory $\vec{R} = \vec{R}_0 + \vec{v}t$,

$$\begin{aligned} \Phi_{0,DC}(\vec{r}') &= \lim_{T \rightarrow \infty} \frac{1}{T} \int_0^T dt \sum_{\vec{g}} \Phi_0(g) \exp[i\vec{g}\cdot(\vec{R}_0 + \vec{v}t + \vec{r}')] \\ &= \sum'_{\vec{g}} \Phi_0(g) \exp[i\vec{g}\cdot(\vec{R}_0 + \vec{r}')], \end{aligned} \quad (33)$$

where the primed summation extends over only

those reciprocal-lattice vectors \vec{g} which are perpendicular to \vec{v} . For channeling parallel to, say, the crystallographic γ axis, the primed sum extends over \vec{g} in the γ plane, whereas for channeling in the γ plane (not along any low index axis), the sum is over \vec{g} on the γ axis.

When the crystal is treated as a homogeneous, isotropic, translationally invariant medium, the first-order, scalar electric potential Φ_1 originating in the linear polarization induced by a point particle of charge $(Z-1)e$ moving with constant velocity \vec{v} , may be written¹⁵

$$\Phi_1(\vec{r}') = \frac{(Z-1)e}{2\pi^2} \int d^3k \exp(i\vec{k}\cdot\vec{r}') \left(\frac{1}{\epsilon(\vec{k}, \vec{k}\cdot\vec{v})} - 1 \right) k^{-2}, \quad (34)$$

where $\epsilon(\vec{k}, \omega)$ is the longitudinal dielectric function of the medium. Here ϵ depends on the magnitude of \vec{k} . In the present calculation a plasmon-pole type of approximation^{15,16} was used for $\epsilon(\vec{k}, \omega)$;

$$\epsilon^{-1} - 1 = \frac{-\omega_p^2}{\omega_p^2 + \omega_b^2 + \beta^2 k^2 + \hbar^2 k^4 / 4m_e^2 - \omega(\omega + i\sigma)}. \quad (35)$$

The parameter ω_p corresponds to the plasma frequency of an electron gas but may be chosen to fit experimental data on the plasmon-like resonance behavior of real metals, semiconductors, or other solids. Similarly, the damping constant σ may also be taken from experiment, as can β , the hydrodynamical velocity of disturbances in the electron gas. The energy $\hbar\omega_b$ may represent an effective band gap in materials like semiconductors. Single-particle effects are accounted for by the presence of the term equal to the square of the kinetic energy, $\hbar^2 k^2 / 2m_e$, of a free electron with momentum $\hbar\vec{k}$. The dielectric constant represented by Eq. (35) satisfies the sum rules

$$\int_0^\infty \omega \text{Im} \left[\epsilon(\vec{k}, \omega) \right] d\omega = \int_0^\infty \omega \text{Im} \left[\frac{-1}{\epsilon(\vec{k}, \omega)} \right] d\omega = \frac{1}{2} \pi \omega_p^2$$

as it must from very general requirements.¹⁷

In the present applications we have chosen $\omega_b = 0$, $\omega_p = 0.949$ a.u. and

$$\beta^2 = \frac{3}{5} v_f^2 = \left(\frac{2}{5} \right) \left(\frac{2}{\pi} \right)^{2/3} \omega_p^{4/3} \hbar^2 / (m_e e)^{4/3} = 0.815$$

a.u.,¹⁵ and have taken the $\sigma \rightarrow 0^+$ limit, representing Au as an electron gas with a plasma frequency of 25.8 eV, chosen from electron energy-loss experiments.¹⁸ The plasmon-pole approximation of Eq. (35) was employed for most of the work carried out in this connection. However, in one instance, the calculation of the $2p_z, 2s$ matrix ele-

ment of Φ_1 , it was possible to employ the Lindhard dielectric constant¹⁹ to represent the response of an electron gas for which $\hbar\omega_p = 25.8$ eV. The difference in matrix elements computed in the two approximations, for $v = 10.45 v_0$, is less than 1%.

Some matrix elements of $-\frac{1}{2}i\hbar\gamma$ (Eqs. 21 and 17) were computed, with the following approximations, to test whether the contribution of this operator to the energies is negligible. It is convenient to write Q in terms of projection operators p (defined above), $q = 1 - p$, $P_c = |\chi_i\rangle\langle\chi_i|$, and $Q_c = 1 - P_c$ (where the domains of the two pairs of operators are wave functions for ions, and for crystals, respectively) as follows:

$$Q = qP_c + pQ_c + qQ_c.$$

The retarded Green's function G_{QQ}^* was replaced by one, G^* , defined as in Eq. (14a) but without $QH'Q$. Then, Eq. (17) for Γ becomes a sum of three terms, corresponding to the three parts of Q above. For the two terms containing Q_c , we ignore the potential U , and we treat the crystal in a plasmon-pole type of approximation, in which energy transfers $\hbar\omega$ and momentum transfers $\hbar k$ to the crystal are related by

$$\hbar\omega = \hbar\omega_p + (\hbar^2/2m_e)k^2,$$

and the generalized oscillator strength sum rule over excited states is used,

$$\sum_{cm} |(m|e^{i\vec{k}\cdot\vec{r}_c}|0)|^2 \hbar\omega_{m0} = V\hbar^2\omega_p^2 k^2 / 8\pi e^2,$$

where V is the normalization volume for the crystal. This model is the same as the one underlying Eq. (35) for the dielectric function when $\omega_b = 0$ and $\beta^2 = \hbar\omega_p/m_e = 0.949$ a.u. Similarly, we treat q space of the ion by compressing the oscillator strength in q space (for transitions from any state in p space) into a single final energy $(\hbar^2/2m_e)k^2$ (relative to the ionization limit of a free ion) for a given momentum transfer $\hbar k$. The q - p transition strength is determined by the generalized oscillator strength sum rule

$$\sum_j |\langle j|e^{i\vec{k}\cdot\vec{r}_a}|i\rangle|^2 \hbar\omega_{ji} = \hbar^2 k^2 / 2m_e, \quad i \leq 5.$$

The calculated values of the real part of $\langle 2s | -\frac{1}{2}i\hbar\gamma | 2s \rangle$ are found to be less in absolute value than the experimental uncertainties in the transition energies, except possibly for C^{5+} , where the calculation gives $-0.029 e^2/a_0$ for $v = 6 v_0$ in the $\langle 100 \rangle$ channel. Because of this, and because the calculation is probably an overestimate (due to assuming too small a q - p transition energy), we neglect

the real part of $-\frac{1}{2}i\hbar\gamma$ in the remainder of this paper.

Calculation of the energies E_i requires diagonalizing the Hamiltonian $H_a - e\Phi_{0,DC} - e\Phi_1$ in the space of five eigenfunctions ($1s, 2s, 2p_x, 2p_y$, and $2p_z$) of the atomic Hamiltonian H_a , taking $\Phi_{0,DC}$ and Φ_1 from Eqs. (33) and (34), respectively. For $pH_a p$, we start with the nonrelativistic hydrogenic Hamiltonian, and subtract a small constant from the $1s$, $1s$ element to correct the energies for relativistic effects other than fine-structure splitting. (The fine-structure splitting is smaller than both the above correction, and the resolution of the present experiment, and is therefore ignored.) The correction is such that the excited eigenvalues of $pH_a p$ are degenerate and have energies above the ground state by the amount of the spectroscopic value of the $2p \ ^2P_{3/2} - 1s \ ^2S$ transition energy in the free ion.

The z axis is oriented along the direction of motion and, in the planar case, the x axis is perpendicular to the channel. It is convenient to integrate over configuration space first, before performing the subsequent sums or integrals indicated.

The results for O^{7+} moving with a velocity⁶ $10v_0$ along the center line of a $\langle 100 \rangle$ axis of gold are shown in Fig. 2. In the middle of the figure is shown the effect that the static crystal potential $\Phi_{0,DC}$ has upon the energies. The $n=2$ states are

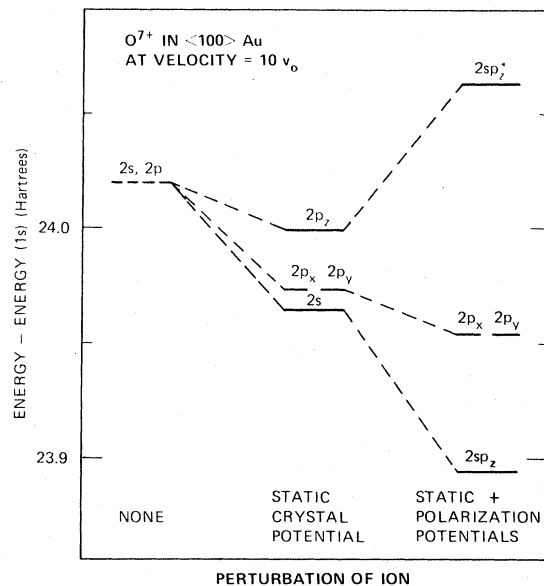


FIG. 2. Energy, relative to the $1s$ state, of four excited states of O^{7+} moving along the center line of a $\langle 100 \rangle$ channel in Au with velocity $10v_0$, according to this theory. Starting on the left, values are for free ions, and for ions with the indicated perturbations.

shifted down slightly by varying amounts with respect to the $1s$ level, as compared with the free-ion energies. As shown in the Appendix, these shifts are approximately proportional to the electron density averaged down the channel center line. We note from the right-hand side of Fig. 2 that the polarization potential Φ_1 also depresses the levels slightly, but its main effect is to mix and split the $2s$ and $2p_z$ levels. This latter is similar to the first-order Stark effect. Because of the ion's motion, the induced electron density tends to lag behind the ion in the form of a wake.^{15,20} The result is an induced field which, in the neighborhood of the ion, is directed opposite to the velocity, and acts to retard the ion. The same field mixes the $2s$ and $2p_z$ levels.

The induced electron density varies too rapidly with position near the ion for a second-order Taylor series expansion to be useful in computing the diagonal matrix elements of Φ_1 , so the latter are not simply proportional to the induced electron density at the center of the ion. However, the $2s$, $2p_z$ matrix element may be estimated within about a factor of 2 (depending on atomic number and velocity) from the stopping power in this model, by approximating the induced field as a constant over the volume of the ion.

Calculated spectral shifts for N^{6+} moving in the midplane of the $\{100\}$ planar channel are shown in Fig. 3, plotted against v^{-2} . The left intercepts of the curves are determined by the static potential $p\Phi_0$, DCp only, and are approximately proportional to electron density in the channel, as shown in the Appendix. The changes in these curves with increasing v^{-2} (decreasing v) are due to the wake. As in the axial case, above, one sees a Stark-type mixing and splitting of the $2s$ and $2p_z$ states by the

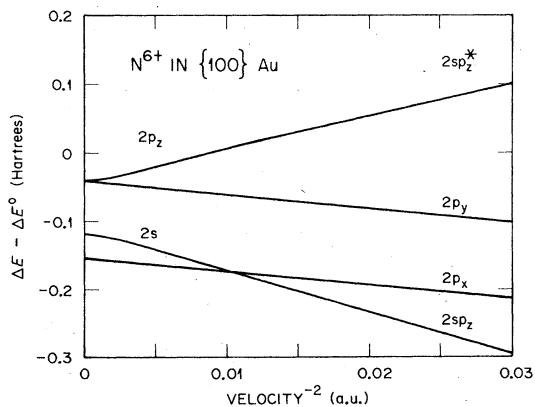


FIG. 3. Transition energies ΔE from $1s$, relative to the transition energy ΔE^0 in free ions, vs the inverse square of ion velocity, for N^{6+} centered in $\{100\}$ planar channels of Au, according to this theory.

wake. We note that the $2p_x$ and $2sp_z$ levels cross, which is allowed on account of the reflection symmetry of the Hamiltonian. For trajectories not in the midplane, this level crossing does not occur.

V. COMPARISON WITH EXPERIMENT

Resonant coherent excitation spectra have been reported from this laboratory.^{3,4} Beams of one-electron ions obtained from the Oak Ridge National Laboratory tandem Van de Graaff accelerator were passed in channeling directions through thin single crystals. Spectra were determined by measuring charge-state populations (charges $Z-1$ and Z) of the collimated emergent beam. Local minima in the curves of count ratios ($Z-1$ to the sum of $Z-1$ and Z counts) versus velocity are evidence of resonance coherent excitation. From the velocities at which these minima occur, the experimental transition energies ΔE have been calculated, using relations

$$\Delta E = \begin{cases} 2\pi\hbar K v/a, & K=1, 2, 3, \dots \text{ for } \langle 100 \rangle \\ 2\pi\hbar K v/\sqrt{3}a, & K=1, 2, 3, \dots \text{ for } \langle 111 \rangle, \end{cases}$$

which follow from Eqs. (25) and (26). The lattice constant a of Au at 25°C is²¹ 4.07897 \AA .

The theoretical values of transition energies ΔE as compared with the free-space values ΔE^0 are plotted as solid curves in Figs. 4–9. The dotted curves are angular frequencies as functions of velocity, Eq. (26), with spectroscopic values²² of ΔE^0 ($2p^2P_{3/2} - 1s^2S$) deducted. At the intersections, the resonance condition Eq. (25) is satisfied. The intersections where dipole selection

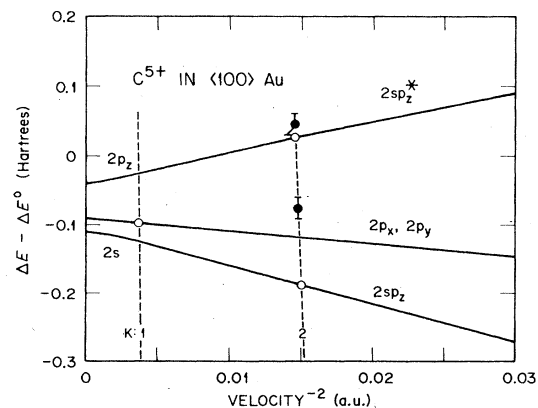


FIG. 4. Transition energies ΔE from $1s$, relative to the transition energy ΔE^0 in free ions, vs the inverse square of ion velocity, for C^{5+} centered in $\langle 100 \rangle$ axial channels of Au. —, this theory; ---, $2\pi\hbar K v/a - \Delta E^0$; O, predicted resonant coherent excitation (RCE); ●, observed RCE (Refs. 3 and 4).

rules^{3,4} are also satisfied, marked with open circles, are where resonant coherent excitation is expected. The experimental points, obtained from minima in the count ratios discussed above, are the filled circles. Most of the experimental curves from which these points come are shown in Ref. 4. We have corrected the experimental velocities for slowing down in the crystal.

The experimental curves of count ratios versus velocity contain rather broad dips, most of which are pointed at the bottom. It is reasonable to assume, as we do, that the minima occur at velocities where ions on centered trajectories come into resonance, as these trajectories are associated with the longest coherence times (and smallest widths). This assumption cannot be strictly true in the case of odd harmonic resonances in a $\langle 100 \rangle$ axial channel, as the odd Fourier components of the field are all zero in the center of this channel.⁴

In Fig. 4 is given a comparison between theory and experiment for excitation of C^{5+} by the second harmonic in the $\langle 100 \rangle$ axial channel. The second harmonic part of the alternating field, as seen by ions on the center line of a $\langle 100 \rangle$ channel, points in the z direction (parallel to the velocity). By symmetry, only the $2sp_x$ and $2sp_x^*$ states of centered ions can be excited by this harmonic.⁴ The ratio of intensities corresponding to exciting these two states, assuming centered ions, should equal approximately the ratio of the squares of the $2p_x$ coefficients in the two states. These coefficients, taken from the calculated eigenvectors of $p(H_a - \Phi_{DC})p$ for C^{5+} at the appropriate velocity, give the result on the basis of the above argument that the intensity of the transition to the lower ($2sp_x$) of these two states should be only 0.36 times that to the higher ($2sp_x^*$) one. However, the two resonances observed experimentally (Fig. 11 of Ref. 4) are of nearly equal strength. Furthermore, as is seen in Fig. 4, the lower experimental resonance has its energy near that calculated for the degenerate $2p_x$ and $2p_y$ states. Therefore, we attribute this lower feature to $2p_x$ and $2p_y$ states, excited in trajectories which are far enough from the channel center line to break the symmetry on which the selection rules discussed above are based. It is not clear why a smaller minimum representing the $2sp_x$ state is not observed, but it may be obscured by the larger feature near it.

Since the transverse component of the alternating field becomes about as large as the longitudinal (or z) component (in the second harmonic) at approximately 0.4 \AA from the channel center line,⁴ the near equality of the intensities of the two observed resonances suggests that transitions in ions at distances of about 0.4 \AA from the center line make significant contributions to the observed

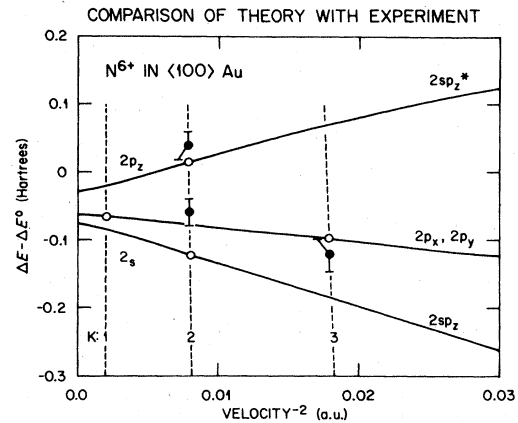


FIG. 5. Transition energies ΔE from $1s$, relative to the transition energy ΔE^0 in free ions, vs the inverse square of ion velocity, for N^{6+} centered in $\langle 100 \rangle$ axial channels of Au. —, this theory; ---, $2\pi\hbar K v/a - \Delta E^0$; O, predicted resonant coherent excitation (RCE); ●, observed RCE (Refs. 3 and 4).

resonances. A similar conclusion was reached previously⁴ from examination of energy-loss spectra.

Similar conclusions are suggested by the second-harmonic resonances in N^{6+} in $\langle 100 \rangle$, Fig. 5. The discussion of calculated intensity ratios versus observed ones carries over quantitatively, and the lower of the pair of minima seen in the second harmonic is attributed to $2p_x$ and $2p_y$. This assignment is consistent with the $2p_x - 1s$ energy measured with the third harmonic, also shown in Fig. 5.

Figure 6 shows agreement between theory and

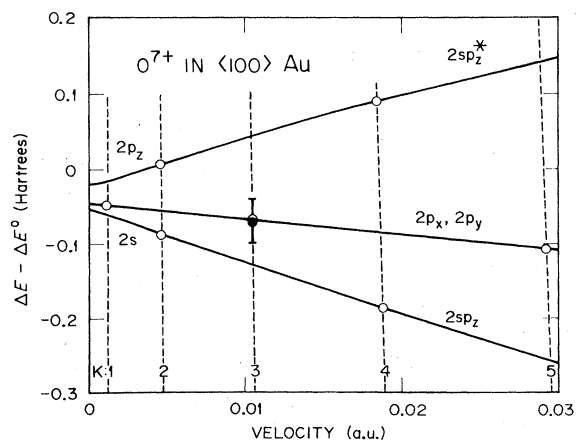


FIG. 6. Transition energies ΔE from $1s$, relative to the transition energy ΔE^0 in free ions, vs the inverse square of ion velocity, for O^{7+} centered in $\langle 100 \rangle$ axial channels of Au. —, this theory; ---, $2\pi\hbar K/a - \Delta E^0$; O, predicted resonant coherent excitation (RCE); ●, observed RCE (Refs. 3 and 4).

experiment for the $2p_x, 2p_y$ level of O^{7+} in $\langle 100 \rangle$ similar to that found for N^{6+} . A second minimum, much smaller than the main one, was omitted from the graph.

The F^{8+} resonance is weak, and its position is difficult to read, as indicated by the large error limits in Fig. 7. The double minimum predicted by the theory is not resolved. The count ratio curve appears to have a very small secondary minimum at a velocity which is (if due to the fourth harmonic) too low for the corresponding ΔE to fit on Fig. 7, but this feature may be due to noise.

Transition energies for C^{5+} and N^{6+} in the $\langle 111 \rangle$ axial channel are shown in Figs. 8 and 9. There are only small differences between the calculated and experimental transition energies. In the case of N^{6+} , the experimental count rate curve shows no evidence for the $2sp_x - 1s$ transition expected to be produced by the sixth harmonic. This is not significant, as the $2sp_x^* - 1s$ resonance observed with this harmonic is quite weak, and the intensity of the missing minimum should be still smaller, by a factor of 3, judging by the relative $2p_x$ characters of the $2sp_x$ and $2sp_x^*$ states.

The $\langle 111 \rangle$ channel is narrower than the $\langle 100 \rangle$ one, with greater average electron density on the center line. Thus, on the basis of Eq. (A3), greater static shifts are anticipated, and both the detailed calculations and the experimental results in Figs. 8 and 9 confirm this point.

VI. CONCLUSIONS

A time-dependent effective-Hamiltonian theory for the electrons of channeled ions has been pro-

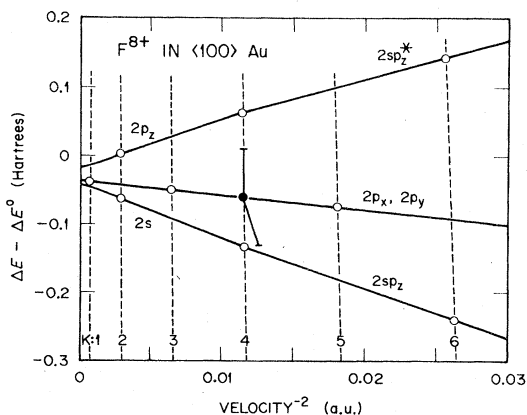


FIG. 7. Transition energies ΔE from $1s$, relative to the transition energy ΔE^0 in free ions, vs the inverse square of ion velocity, for F^{8+} centered in $\langle 100 \rangle$ channels of Au. —, this theory; ---, $2\pi\hbar K/a - \Delta E^0$; O, predicted resonant coherent excitation (RCE); ●, observed RCE (Refs. 3 and 4).

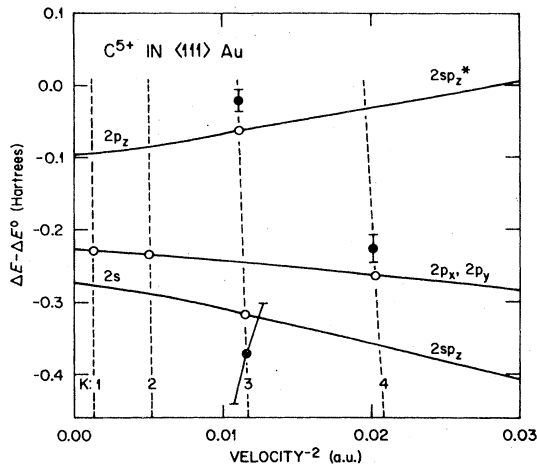


FIG. 8. Transition energies ΔE from $1s$, relative to the transition energy ΔE^0 in free ions, vs the inverse square of ion velocity, for C^{5+} centered in $\langle 111 \rangle$ axial channels of Au. —, this theory; ---, $2\pi\hbar K/\sqrt{3}a - \Delta E^0$; O, predicted resonant coherent excitation (RCE); ●, observed RCE (Refs. 3 and 4).

posed, and transition energies have been calculated for swift one-electron ions centered in various channels of Au. Such calculations require expectation values of both the static (or unperturbed) potential in the crystal and the wake potential induced by a moving point charge. An approximation in terms of the mean electron density in the channel center is suggested for possible future

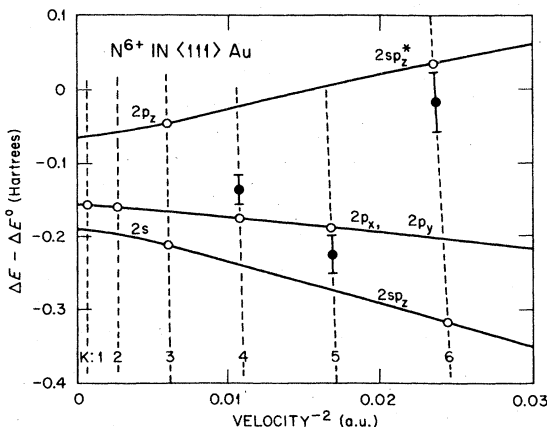


FIG. 9. Transition energies ΔE from $1s$, relative to the transition energy ΔE^0 in free ions, vs the inverse square of ion velocity, for N^{6+} centered in $\langle 111 \rangle$ axial channels of Au. —, this theory; ---, $2\pi\hbar K/\sqrt{3}a - \Delta E^0$; O, predicted resonant coherent excitation (RCE); ●, observed RCE (Refs. 3 and 4).

use in lieu of the full static potential.

The static potential was obtained from a relativistic quantum mechanical calculation for an Au atom with Wigner-Seitz boundary conditions, averaged over vibrations, and the polarization was estimated from dielectric theory.

The results are in reasonably good quantitative agreement with recent measurements of resonant coherent excitation. It is suggested that improvement in the agreement requires that consideration be given in the calculation to ions whose trajectories are not centered in the channel, and to an improved treatment of the polarization wake.

ACKNOWLEDGMENTS

We thank V. E. Anderson for providing plots of the electron wake, and C. W. Nestor, Jr., for supplying a punched card deck of the potential in Au, and we thank both of them for performing some of the computations. One of us (O.H.C.) acknowledges helpful discussions with I. L. Thomas, C. K. Johnson, S. Datz, and R. L. Becker. This work was sponsored by the Division of Chemical Sciences, Office of Basic Energy Sciences, U.S. Department of Energy under Contract No. W-7405-eng-26 with the Union Carbide Corporation.

APPENDIX

Relationships between the electron density and the energy shifts due to the static potential $\Phi_{0,DC}$ are derived in this Appendix.

The average $\Phi_{0,DC}$ of the potential Φ_0 along the direction of a crystallographic axis may be written as an expansion in cylindrical coordinates:

$$\bar{\Phi}_{0,DC} = \bar{\Phi}(\rho) + \sum_{m \neq 0} \Phi_m(\rho) \exp(im\phi),$$

where ρ is the distance from a channel center line, and ϕ is the azimuthal angle. For $\langle 111 \rangle$ and $\langle 100 \rangle$ axial channels, the above sum extends over only those m values which are integral multiples of 3 and 4, respectively, by symmetry. For an ion on the channel center line, the matrix elements, in a basis of s and p electronic states, of $\exp(\pm im\phi)$ are all zero for $m \geq 3$. Therefore, given an s and p basis, $\bar{\Phi}(\rho)$ is the only part of $\Phi_{0,DC}$ which effects ions centered in $\langle 111 \rangle$ or $\langle 100 \rangle$ axial channels.

Upon averaging both sides of Poisson's equation, one finds

$$\frac{1}{\rho} \frac{\partial}{\partial \rho} \left(\rho \frac{\partial}{\partial \rho} \right) \bar{\Phi}(\rho) = -4\pi\bar{n}(\rho), \quad (\text{A1})$$

where \bar{n} is the expectation value (for the state χ of the crystal) of the charge density, averaged down

the axis and over azimuthal angle. It follows that the coefficients of the Taylor expansion of $\bar{\Phi}$ about the channel center line,

$$\bar{\Phi}(\rho) = \bar{\Phi}(0) - \pi\bar{n}(0)\rho^2 - \dots - \frac{\pi}{m^2(2m-2)!} \left. \frac{\partial^{2m-2}\bar{n}(\rho)}{\partial \rho^{2m-2}} \right|_{\rho=0} \rho^{2m} - \dots, \quad (\text{A2})$$

are proportional to the average charge density \bar{n} and its derivatives at $\rho=0$. Dropping terms of fourth and higher order from Eq. (A2) leads to the following approximation for the static first-order contribution to spectral shifts for ions on the channel axis, in terms of the average down the channel center line, \bar{n}_e , of the electron density:

$$\begin{aligned} \Delta E_{\text{stat}}(j-1s) - \Delta E^0(j-1s) & \\ & \simeq -\pi\bar{n}_e[\langle j|\rho^2|j\rangle - \langle 1s|\rho^2|1s\rangle] \\ & = \begin{cases} -26\pi Z^{-2}\bar{n}_e, & \text{for } 2s \\ -22\pi Z^{-2}\bar{n}_e, & \text{for } 2p_x, 2p_y \\ -10\pi Z^{-2}\bar{n}_e, & \text{for } 2p_z, \end{cases} \quad (\text{A3}) \end{aligned}$$

where ΔE_{stat} and ΔE^0 are, respectively, the energy spacings between the two states indicated, with and without the inclusion of the static potential $p\Phi_{0,DC}p$ in the Hamiltonian (but without the polarization potential). Values of $\Delta E_{\text{stat}} - \Delta E^0$ given by Eqs. (A3) would be exact if the density $\bar{n}(\rho)$ did not vary with ρ , and are within 2% of the values computed using the full static potential $p\Phi_{0,DC}p$, for O^{7+} in Au $\langle 100 \rangle$. Agreement tends to be poorer for lower- Z ions and for narrower channels.

A similar derivation for planar channeling yields the following relation between the averages $\Phi_{0,DC}(x)$ and $\bar{n}(x)$, of the potentials and charge densities, over the y - z plane, as a function of displacement x from the midplane of the channel:

$$\begin{aligned} \Phi_{0,DC}(x) = \Phi_{0,DC}(0) - 2\pi\bar{n}(0)x^2 - \dots \\ - \frac{4\pi}{(2m)!} \left. \frac{\partial^{2m-2}\bar{n}(x)}{\partial x^{2m-2}} \right|_{\rho=0} x^{2m} - \dots \quad (\text{A4}) \end{aligned}$$

Dropping terms of fourth and higher order leads to the following approximation for the static contribution to spectral shifts for ions on the channel midplane in terms of the average over the midplane, \bar{n}_e , of the electron density:

$$\begin{aligned} \Delta E_{\text{stat}}(j-1s) - \Delta E^0(j-1s) & \\ & = \begin{cases} -26\pi Z^{-2}\bar{n}_e, & \text{for } 2s \\ -34\pi Z^{-2}\bar{n}_e, & \text{for } 2p_x \\ -10\pi Z^{-2}\bar{n}_e, & \text{for } 2p_y, 2p_z \end{cases} \quad (\text{A5}) \end{aligned}$$

The above expressions would be exact if the density $\bar{n}(x)$ did not vary with x , and give results within 18% of the values computed for O^{7+} in the {100} planar channel of Au.

The approximations derived in this Appendix

were not used in the calculations reported in this work. They are included both for possible future use, and as evidence that the energy shifts due to the static potential are determined mainly by the electron density in the center of the channel.

-
- ¹D. S. Gemmell, Rev. Mod. Phys. 46, 129 (1974); D. V. Morgan, editor, *Channeling Theory, Observation and Applications* (Wiley, London, 1973).
- ²G. J. Kutcher and M. H. Mittleman, Phys. Rev. A 11, 125 (1975).
- ³S. Datz, C. D. Moak, O. H. Crawford, H. F. Krause, P. F. Dittner, J. Gomez del Campo, J. A. Biggerstaff, P. D. Miller, P. Hvelplund, and H. Knudsen, Phys. Rev. Lett. 40, 843 (1978).
- ⁴C. D. Moak, S. Datz, O. H. Crawford, H. F. Krause, P. F. Dittner, J. Gomez del Campo, J. A. Biggerstaff, P. D. Miller, P. Hvelplund, and H. Knudsen, Phys. Rev. A 19, 977 (1979).
- ⁵V. V. Okorokov, JETP Lett. 2, 111 (1965); Yad Fiz. 2, 1009 (1965), [Sov. J. Nucl. Phys. 2, 719 (1966)].
- ⁶The Bohr velocity $v_0 = e^2/\hbar = 2.187\ 69 \times 10^6$ m/sec; $\frac{1}{2}v_0^2 = 2.480\ 13 \times 10^{-2}$ MeV/amu.
- ⁷R. G. Newton, *Scattering Theory of Waves and Particles* (McGraw-Hill, New York, 1966), p. 150.
- ⁸Since the interaction H' increases with orbital radius, H' increases with principal quantum number of the ion, and decreases with atomic number.
- ⁹F. Bell, H.-D. Betz, H. Panke, and W. Stehling, J. Phys. B 9, L443 (1976).
- ¹⁰D. H. Jakubassa, J. Phys. C 10, 4491 (1977).
- ¹¹We are assuming the Hermitian part of $-\frac{1}{2}i\hbar\gamma$ to be negligible, in line with the discussions following Eq. (17) and in Sec. IV. The anti-Hermitian part of this operator broadens the resonances, but does not shift them.
- ¹²N. F. M. Henry and K. Lonsdale, *International Tables for X-Ray Crystallography* (Kynoch, Birmingham, 1952), Vol. I, p. 517.
- ¹³T. C. Tucker, L. D. Roberts, C. W. Nestor, Jr., T. A. Carlson, and F. B. Malik, Phys. Rev. 178, 998 (1969).
- ¹⁴V. Synecek, H. Chessin, and M. Simerska, Acta Crystallogr. A 26, 108 (1970).
- ¹⁵See, e.g., J. Neufeld and R. H. Ritchie, Phys. Rev. 98, 1632 (1955); and R. H. Ritchie, W. Brandt, and P. M. Echenique, Phys. Rev. B 14, 4808 (1976), and references given therein.
- ¹⁶B. I. Lundqvist, Phys. Konden. Mater. 6, 206 (1967); L. Hedin and S. Lundqvist, Solid State Phys. 23, 84 (1969); A. W. Overhauser, Phys. Rev. B 3, 1888 (1971).
- ¹⁷D. Pines and P. Nozieres, *The Theory of Quantum Liquids* (Benjamin, New York, 1966), pp. 204 ff.
- ¹⁸J. Daniels, C. v. Festenburg, H. Raether, and K. Zeppenfeld, in *Springer Tracts in Modern Physics* (Springer, Berlin, 1970), Vol. 54.
- ¹⁹J. Lindhard, K. Dan. Vidensk. Selsk. Mat.-Fys. Medd. 28, No. 8 (1954).
- ²⁰N. Bohr, K. Dan. Vidensk. Selsk. Mat.-Fys. Medd. 18, No. 8 (1948).
- ²¹J. D. H. Donnay and H. M. Ondik, *Crystal Data Determinative Tables*, 3rd ed. (U.S. Department of Commerce, Washington, D. C., 1973), Vol. II, p. C-44.
- ²²R. L. Kelly and L. J. Palumbo, *Atomic and Ionic Emission Lines Below 2000 Angstroms*, NRL Report No. 7599 (Naval Research Laboratory, Washington, D. C., 1973).